Science of the Total Environment 595 (2017) 451–460

Contents lists available at ScienceDirect

Science of the Total Environment

journal homepage: www.elsevier.com/locate/scitotenv

Continued decrease of open surface water body area in Oklahoma during 1984–2015

Zhenhua Zou [a], Jinwei Dong [b], Michael A. Menarguez [a,c], Xiangming Xiao [a,d,*], Yuanwei Qin [a], Russell B. Doughty [a], Katherine V. Hooker [e], K. David Hambright [e]

[a] Department of Microbiology and Plant Biology, Center for Spatial Analysis, University of Oklahoma, Norman, OK 73019, USA
[b] Key Laboratory of Land Surface Pattern and Simulation, Institute of Geographic Sciences and Natural Resources Research, CAS, Beijing 100101, China
[c] LinkedIn, LLC, San Francisco, CA 94105, USA
[d] Ministry of Education, Key Laboratory of Biodiversity Science and Ecological Engineering, Institute of Biodiversity Science, Fudan University, Shanghai 200433, China
[e] Plankton Ecology and Limnology Laboratory, Department of Biology, University of Oklahoma, Norman, OK 73019, USA

HIGHLIGHTS

- All Landsat 5/7 images were used to generate water body frequency maps.
- Water body variability in maximum, year-long, seasonal, and average water extents
- Both water body area and number decreased significantly during 1984–2015.

GRAPHICAL ABSTRACT

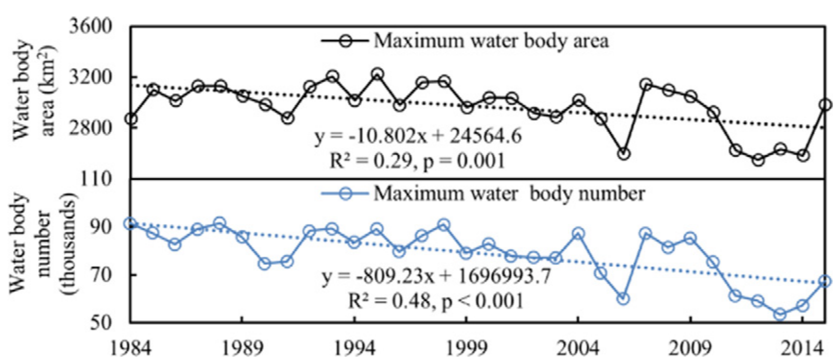

ARTICLE INFO

Article history:
Received 21 January 2017
Received in revised form 27 March 2017
Accepted 28 March 2017

Editor: D. Barcelo

Keywords:
Surface water body
Mapping
Landsat
Climate change

ABSTRACT

Oklahoma contains the largest number of manmade lakes and reservoirs in the United States. Despite the importance of these open surface water bodies to public water supply, agriculture, thermoelectric power, tourism and recreation, it is unclear how these water bodies have responded to climate change and anthropogenic water exploitation in past decades. In this study, we used all available Landsat 5 and 7 images (16,000 scenes) from 1984 through 2015 and a water index- and pixel-based approach to analyze the spatial-temporal variability of open surface water bodies and its relationship with climate and water exploitation. Specifically, the areas and numbers of four water body extents (the maximum, year-long, seasonal, and average extents) were analyzed to capture variations in water body area and number. Statistically significant downward trends were found in the maximum, year-long, and annual average water body areas from 1984 through 2015. Furthermore, these decreases were mainly attributed to the continued shrinking of large water bodies (>1 km^2). There were also significant decreases in maximum and year-long water body numbers, which suggested that some of the water bodies were vanishing year by year. However, remarkable inter-annual variations of water body area and number were also found. Both water body area and number were positively related to precipitation, and negatively

* Corresponding author at: Department of Microbiology and Plant Biology, University of Oklahoma, 101 David L. Boren Blvd., Norman, OK 73019-5300, USA.
E-mail address: xiangming.xiao@ou.edu (X. Xiao).
URL: http://www.eomf.ou.edu (X. Xiao).

http://dx.doi.org/10.1016/j.scitotenv.2017.03.259

related to temperature. Surface water withdrawals mainly influenced the year-long water bodies. The smaller water bodies have a higher risk of drying under a drier climate, which suggests that small water bodies are more vulnerable under climate-warming senarios.

1. Introduction

Climate change and increased climate variability can strongly impact surface water resources (Aherne et al., 2006; Ferguson and Maxwell, 2012; Tulbure et al., 2016), causing dramatic intra-annual and inter-annual water variability (Hall et al., 2014; Mercier et al., 2002), which has been shown to have wide-ranging consequences on human societies and ecosystems (Bates et al., 2008; Brown and Lall, 2006). Previous studies using remote sensing approaches have documented strong relationships between water body extent (area and number) with both climate variability and anthropogenic impacts of water resources (Liu et al., 2013; Pekel et al., 2016; Tao et al., 2015; Tulbure and Broich, 2013; Tulbure et al., 2014).

Water body monitoring with remote sensing techniques has advanced along with an increase in freely available, high-resolution satellite data. Many approaches were developed primarily based on Landsat spectral bands, water indices and decision tree classification algorithms (Fisher et al., 2016; Mueller et al., 2016; Tulbure and Broich, 2013). First, many water indices were defined to delineate water bodies with emphases on different features (Bhagat and Sonawane, 2011; Boland, 1976; Crist, 1985; Gond et al., 2004; McFeeters, 1996; Rouse et al., 1974; Shine and Mesev, 2007; Xiao et al., 2002; Xu, 2006) (see supplementary online material 1 (SOM 1)). For example, McFeeters (1996) defined the Normalized Difference Water Index (NDWI) using green and near infrared band to delineate open water features. Xu (2006) modified the NDWI into mNDWI by replacing the near infrared band with short-wave infrared band to suppress the noise of built-up land. mNDWI is one of the most widely used water indices due to its good performance in water body delineation across diverse landscapes (Du et al., 2012; Feyisa et al., 2014; Hui et al., 2008; Ogilvie et al., 2015; Tao et al., 2015).

Second, previous remote sensing approaches have inconsistent capabilities of capturing water body variability. Many surface water bodies have strong intra-annual dynamics, during for example, wet and dry seasons (Alsdorf et al., 2007; Tulbure and Broich, 2013). But some studies estimated water body extent from satellite images gathered at a single time of the year, typically in the wet season (Feng et al., 2011; Homer et al., 2015; Liu et al., 2013). However, it is difficult to define the proper period due to uncertainties in intra-annual variability of climate and anthropogenic effects. Some studies compared the difference of water body area between the same time of selected years to indicate the increasing or decreasing trends of water body area among those years (Du et al., 2012; Homer et al., 2015; Necsoiu et al., 2013; Tao et al., 2015). However, due to the strong inter-annual dynamics of open surface water bodies (Hall et al., 2014; Mercier et al., 2002; Tulbure et al., 2016), the selection of different years for comparison could lead to very different results and inaccurate inference of trends in water body area and number. Thus, a comprehensive analysis considering different phases or extents of surface water bodies is important. To get a more complete picture of water body variability in Oklahoma, USA, we explored four indicators of surface water body extents based on the annual water body frequency: 1) the maximum water body extent in a given year, 2) the persistent year-long water body extent, 3) seasonal changes in water body area, which is the difference between the maximum and year-long water body extents, and 4) the annual average water body extent.

Oklahoma is located in a climatic transition zone characterized as sub-humid in south and east to cold and dry in north and west, which causes a widely variable seasonal fluctuation in weather (Gibson, 1981). The few natural water bodies in Oklahoma are temporary oxbows and playas (Johnson and Luza, 2008), but >200 large reservoirs have been built in Oklahoma to meet current and projected water demand for human society and ecosystems (OWRB and ODWC, 2015). Between 1985 and 2010, 47% of the total annual water withdrawals in Oklahoma came from these open surface water bodies (U.S. Geological Survey, 2010). Some water-use sectors rely more heavily on open surface water bodies as a percentage of their total water use than others, especially thermoelectric power (99%), public water supply (82%) and livestock (65%) (U.S. Geological Survey, 2010). From 1980 to 2009, Oklahoma's soil moisture continuously declined due to decreased precipitation and increased land surface net radiation and temperature (Lin et al., 2013). The prevailing climate models have predicted more frequent and intense droughts in the Southern Great Plains due to changes in precipitation intensity and frequency (Shafer et al., 2014). In the context of climate change and variability, changes in water body area and number would undoubtedly affect human society and ecosystems. However, these questions have not been well addressed because studies on this subject are limited in Oklahoma. It is still unclear how open surface water bodies, mostly manmade, have and will respond to a changing climate.

The objective of this study was to investigate the spatial-temporal dynamics of open surface water bodies and analyze their relationship with climate variability and anthropogenic water exploitation in Oklahoma. We used all of the Landsat 5 and 7 surface reflectance images and a water index- and pixel-based algorithm to detect surface water body changes from 1984 through 2015. Four water body extent maps (maximum, year-long, seasonal, and average) for each year were generated based on annual water body frequency at the pixel level, which better represented water body status in a more comprehensive way. We analyzed the trends and variations of both water body area and number of four different water body extents. With a continuous long record of water body area and number in a climatic transition zone of widely variable weather, the relationship between water body variability, climate factors (precipitation and temperature) and anthropogenic water exploitation (surface water withdrawals) were analyzed. This study aimed to develop a systematic approach for monitoring changes in the area and number of water bodies in Oklahoma using remote sensing, and to understand the effects of climate change and water exploitation on water bodies. This study provided useful implications for future adaption to climate change in agricultural, industrial, and environmental protection sectors.

2. Materials and methods

2.1. Study area

Oklahoma is located in the south central United States (SOM 2), with an area of ~181,000 km^2 (U.S. Census Bureau, 2010). Its altitude decreases gradually from the high plains in the west to the forest dominated landscape of the east. Oklahoma's temperature decreases from south to north while its precipitation decreases from east to west. The statewide long-term annual average temperature and annual total precipitation are 15.4 °C and 857.8 mm respectively (Oklahoma Climatological Survey, 2016). The 147 most imperative lakes and reservoirs, featured in *Lakes of Oklahoma* (OWRB and ODWC, 2015), were built between 1902 and 1997. Ninety-four percent of these water bodies existed before the beginning (1984) of our study period. Oklahoma has approximately 3000 lakes, reservoirs, and ponds that are 4 ha or more in size. Of these, there are 53 lakes that span >400 ha (OWRB and ODWC, 2015).

2.2. Data

We made use of the Landsat 5 and 7 surface reflectance data archive in Google Earth Engine (GEE) (Google Earth Engine, 2017), which is about 16,000 images of our study area. These datasets were computed from the Landsat standard Level 1 Terrain-corrected (L1T) images in USGS using Landsat Ecosystem Disturbance Adaptive Processing System (LEDAPS) algorithms (Department of the Interior U.S. Geological Survey, 2012). Observations of unacceptable quality, caused by invalid pixels, cloud, and snow, were excluded in our calculation based on the corresponding masks in the 8-bit quality band in each image. The availability of high quality observations was crucial to the generation of the annual water body maps. Landsat tiles and the total image number of each tile in the last 32 years were shown in Fig. 1a. The numbers of available images in each year are shown in Fig. 1b, and the distribution of average annual good observations of all pixels from 1984 through 2015 are shown in Fig. 1c. More than 99.9% of the pixels had 14 or more good observations per year. On average, there were about 25 good observations per pixel in a year. Total observations, total good observations, and percentage of good observations by pixel in 2015 and 1984 through 2015 were shown in supplementary online material 3 (SOM 3).

2.3. Methods

2.3.1. Algorithms to identify open surface water bodies

Despite the advantage of mNDWI over NDWI in the remote sensing of water bodies (Feyisa et al., 2014; Ji et al., 2009; Xu, 2006), the mNDWI approach still has commission error in those mixed pixels of water and other land cover types. In particular, vegetation over a wet surface is one of the major causes for commission error in open surface water body mapping (Santoro et al., 2015). In this study, we combined mNDWI and vegetation indices (NDVI and EVI) to reduce the effects of vegetation on water body mapping algorithm (SOM 4), which has been addressed in our previous studies (Dong et al., 2015; Xiao et al., 2006; Xiao et al., 2005). Specifically, we detected only pixels with water signal that was stronger than the vegetation signal as actual water pixels (mNDWI > NDVI or mNDWI > EVI). In order to further remove the noise caused by vegetation, EVI was applied to exclude the wetland pixels with vegetation (EVI < 0.1). Therefore, only those pixels that met the criteria ((mNDWI > NDVI or mNDWI > EVI) and (EVI < 0.1)) were classified as open surface water body pixels. The remaining pixels were classified as non-water pixels (SOM 5). Two case studies showing water detection in built-up land and vegetated area were included in the supplementary online material 6 (SOM 6). This method was

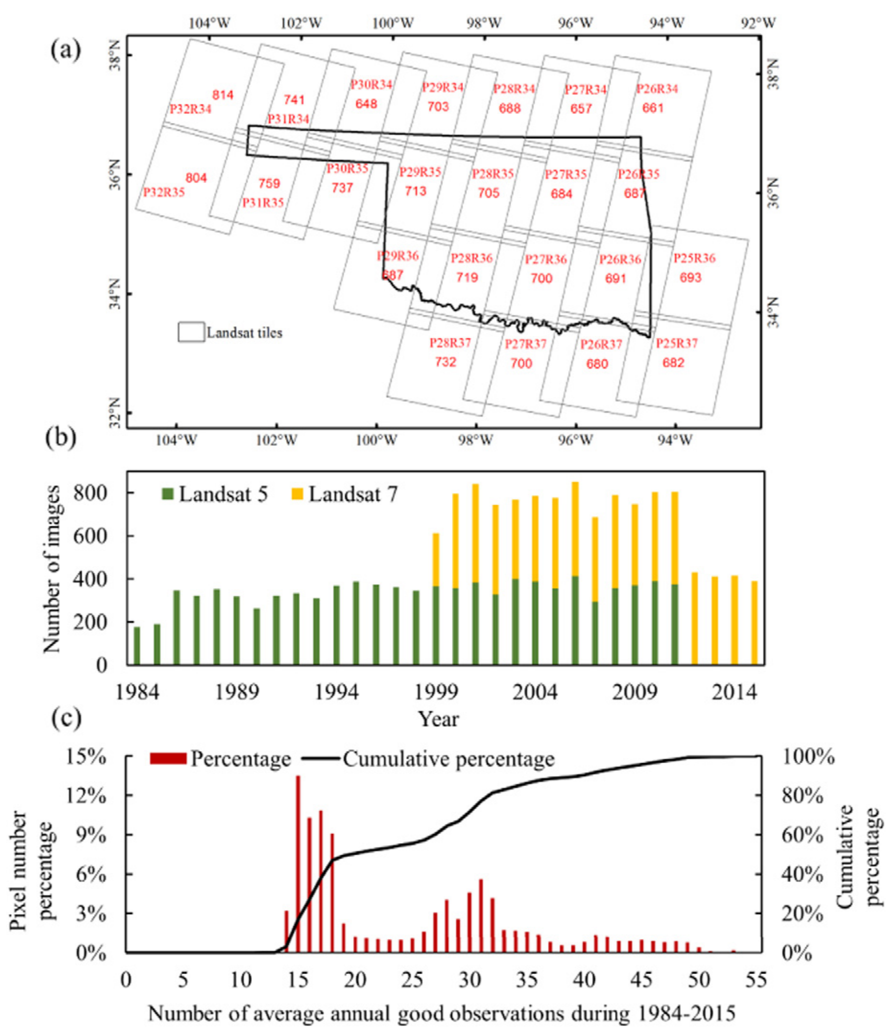

Fig. 1. Landsat data. (a) Landsat tiles and total Landsat 5 and 7 image numbers of each tile from 1984 through 2015, (b) total Landsat 5 and 7 images of the study area in each year, (c) distribution of the average annual good observations from 1984 through 2015, including pixel number percentages of good observations in red bars and cumulative percentages in black curve.

validated using 1 m spatial resolution images as ground reference data in the platform of ArcMap 10.3.1, and the resultant maps of open surface water body had reasonable accuracy (SOM 7).

We used these mapping methods and GEE cloud-computing platform to identify open surface water bodies on all of the 16,000 Landsat images during 1984–2015. For each pixel, we counted the number of observations within a year it was identified as open surface water body, and then divided it by the total number of good observations in that year. We termed the resultant ratio as water body frequency. When the pixel had an annual water body frequency greater than or equal to 0.25, it was classified as effective open surface water pixels. This ≥0.25 frequency limit was chosen because we need to reduce the potential error from the uncertainty in image data quality flags and other small probability problems in image preprocessing (SOM 8). All of the effective open surface water pixels in a year formed the maximum water body extent. Water pixels with an annual water body frequency greater than or equal to 0.75 were classified as year-long water pixels since they have water most of the year. The remaining water pixels, with a water body frequency spanning from 0.25 to 0.75, were classified as seasonal water pixels. For each year, we generated annual maps of maximum water bodies (water body frequency ≥ 0.25%), year-long water bodies (water body frequency ≥ 75%), and seasonal water bodies (25% ≤ water body frequency < 75%) respectively, and then calculate the areas of maximum, year-long and seasonal water bodies correspondingly. Annual average water body area is calculated as a product of all the effective water body pixels and the length of water body (water body frequency) (SOM 9).

We also compared these resultant maps with previous studies for the purpose of inter-comparison. Since most of the available water body data and maps were static or in a specific year (Lehner and Döll, 2004; Verpoorter et al., 2014), we used the annual maximum water body extent in 2000, 2001, 2006, and 2011 to compare with the Global Inland Water (GIW) dataset of 2000 (Feng et al., 2016), National Land Cover Database (NLCD) of 2001 (Homer et al., 2004; Homer et al., 2007; Vogelmann et al., 2001), NLCD of 2006 (Fry et al., 2011), and NLCD of 2011 (Homer et al., 2015) (SOM 10).

2.3.2. Analysis of inter-annual variations and trends of open surface water bodies

The area of maximum, year-long, seasonal, and annual average water body extent in all years (1984–2015) were calculated. Their inter-annual variations during 1984–2015 were analyzed using anomaly analysis while their changing trends were analyzed through linear regression analysis. Water pixels adjacent to each other in the maximum and year-long water body raster maps were merged and converted into vectors respectively. The number of maximum and year-long water bodies in each of the last 32 years was counted and their inter-annual variations and changing trends from 1984 through 2015 were also analyzed through anomaly and linear regression analysis.

2.3.3. Effects of climate and water exploitation on the numbers and areas of open surface water bodies

Multiple linear regression analyses were conducted to explore the relationship between climate, anthropogenic water exploitation, and the variability in the number and area of water bodies. The dependent regression variables of the six regression models were maximum water body area and number, year-long water body area and number, seasonal water body area, and annual average water body area from 1985 through 2015. The climate factors included statewide annual total precipitation and annual average temperature from the Oklahoma Climatological Survey (McPherson et al., 2007). The water exploitation was represented by the statewide annual surface water withdrawal, data on which is gathered every 5 years by U.S. Geological Survey (U.S. Geological Survey, 2010). This surface water withdrawal data was interpolated into annual water withdrawal data spanning from 1985 through 2015 (SOM 11). Water body condition of current year changes from the water body condition of the previous year because of the legacy effect. Thus, the dependent variable in the previous year of each model was used as an independent variable of the subsequent year, serving as the base of water body change in the subsequent year.

3. Results

3.1. Characterizing spatial pattern of open surface water bodies in 2015 and 1984–2015

There were 3.3 million water pixels in both the annual water body frequency map of 2015 and the cumulated water body frequency map of 1984–2015, which represented a maximum water body extent of 2980 km^2 and accounted for ~1.6% of the entire state of Oklahoma (Fig. 2a–b). The distribution of different water body frequency levels of 2015 and 1984–2015 (Fig. 2c–d) showed that about 70% of the water pixels had a water body frequency greater than or equal to 0.75. These water pixels formed the interior portions of large lakes, water reservoirs, and major rivers that were able to maintain water throughout the year. However, water at the shallow edges of these large water bodies would dry up at times due to fluctuations in the water level. For example, the center of Keystone Lake (Fig. 2a–b insets) had water body frequency values close to 1, which meant that it always had water in the deepest part of the lake. The upper part of the lake had water body frequency values around 0.7, which indicated that portion of Keystone Lake could dry up at times and was not very deep. The water body frequency values where the river joined the lake were below 0.5, which indicated that this area only had water during periods of high precipitation and that these portions of the lake were shallow. A large number of small water bodies had a low water body frequency, meaning that they only existed for several months during the wet season or became so small that they could not be detected. The number of water pixels observed in each of the last 32 years was distributed across 8 water body frequency levels in Fig. 2e. The majority of water body pixels had a high water body frequency. There were also some inter-annual variations among different water body frequency levels.

Out of the 3.3 million water pixels in 2015 (SOM 12), there were about 2.3 million year-long water body pixels, which formed the central part of large lakes, reservoirs, and major rivers. The remaining 1.0 million pixels indicated seasonal water bodies, which were comprised of small ponds, minor rivers, and the edges of large water bodies. In 2015, the maximum water body area was 70% year-long and 30% seasonal.

3.2. Inter-annual variation of open surface water bodies during 1984–2015

The maximum, year-long, seasonal and average water body areas showed similar patterns of variation from 1984 through 2015, which were also similar to the variability of precipitation (Fig. 3). The annual maximum water body area from 1984 through 2015 varied between 2548 and 3224 km^2, which was 14% below to 9% above its average value (~2966 km^2). The year-long water body areas varied between −12% and 9% of its average value (2302 km^2), while the seasonal water body areas had the largest variability, from 23% below to 34% above its average value (665 km^2). The annual average water body area best described the average water body extent within one year since it considered the length of water existence of all effective water pixels. The annual average water body area in the last 32 years varied between 2205 and 2758 km^2, which was 12% below to 9% above its mean value (2520 km^2). Statistically significant downward trends were found in the maximum water body areas ($R^2 = 0.29$, $p = 0.001$), year-long water body areas ($R^2 = 0.28$, $p = 0.002$), and annual average water body areas ($R^2 = 0.37$, $p < 0.001$) in the last 32 years (Fig. 3). These downtrends indicated shrinkage of total, statewide water body area. According to the linear regression model, the

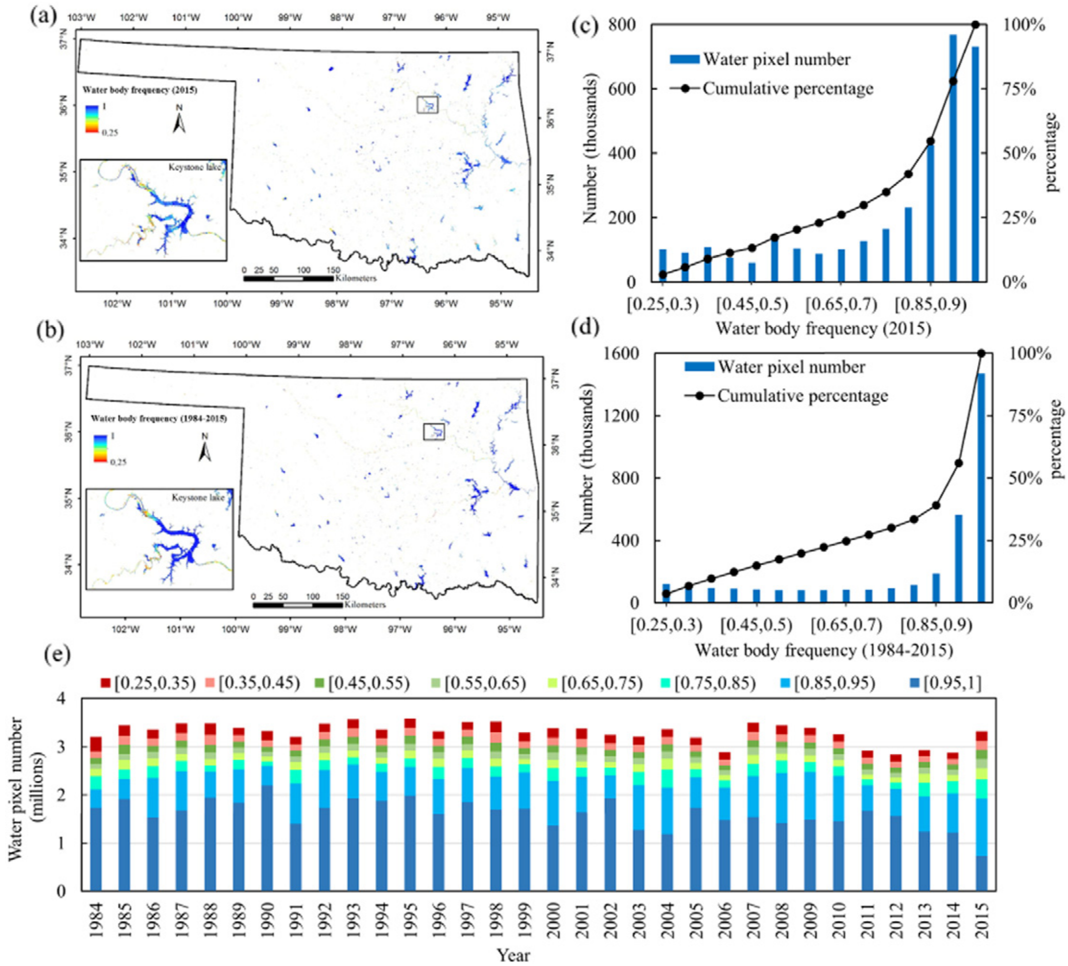

Fig. 2. Water body frequency distribution in Oklahoma. Water body frequency map of 2015 (a) and 1984–2015 (b). The distribution of different water body frequency levels with a bin of 0.05 in 2015 (c) and 1984–2015 (d). Distribution of different water body frequency levels with a bin of 0.1 in 32 years (e).

statewide annual average water body area shrank 10 km^2 each year over the last three decades (Fig. 3d).

The number of maximum and year-long water bodies showed similar patterns of variation from 1984 through 2015 (Fig. 4), which again were similar with those of water body area variations (Fig. 3). The annual maximum water body number in the last 32 years varied between 54,000 and 92,000, which was 32% below to 16% above the average value (79,000). The average year-long water body number from 1984 through 2015 was 36,000, varying between 24,000 and 45,000, which was 33% below to 25% above its average. Statistically significant downward trends were found in the maximum water body numbers ($R^2 = 0.48$, $p < 0.001$) and year-long water body numbers ($R^2 = 0.28$, $p = 0.002$) over the last 3 decades. These decreasing trends in water body number indicated that some water bodies may be disappearing annually.

All of the water bodies in the maximum water extent of each year were classified into 10 ranges based on water body size. The distribution of water body number and area in different classifications were shown in Fig. 5a–b. On average, the number of water bodies larger than 100 ha was only about 138, which made up ~0.18% of the total number of water bodies. However, these larger water bodies contributed 80% of the total water body area on average. The inter-annual variation in area of these large water bodies contributed ~68% of the statewide water body area variation. In comparison, water bodies smaller than 0.5 ha accounted for 77% of the total number of water bodies on average, but they comprised only 3.6% of the total water body area. These small water bodies accounted for ~71% of the statewide inter-annual variation in the number of water bodies. Therefore, variability in water body area was influenced most by the large water bodies, and the variation in the number of water bodies statewide was mainly contributed by the small water bodies.

3.3. Effects of climate and anthropogenic water exploitation on the inter-annual variability of open surface water bodies during 1984–2015

3.3.1. Effects of precipitation, temperature, and water withdrawal on the variability of open surface water bodies

Multiple linear regression was performed with SPSS Statistics 19 using the "stepwise" method for explanatory variable selection. The variance inflation factor (VIF) was used as the collinearity index. The VIFs for all input explanatory variables of each model were below 2.4 (SOM 13). The results of multiple linear regression analysis were shown in Table 1. Precipitation had statistically significant positive effects on all six analyses. Precipitation is the major water source for Oklahoma open surface water bodies. Basically, more precipitation leads to more water bodies and a larger water body area. Temperature had statistically significant negative effects on the annual average water body area, year-long water body area and number. Higher temperature will increase evaporation in addition to other factors, such as higher wind speed, lower concentration of water vapor in the air, lower air pressure, larger surface area etc. Higher temperature may also increase agricultural water demands. Thus, higher temperature may reduce water body area and number. Surface water withdrawal had negative effects on the annual average water body area, year-long water body area and number. In Oklahoma, total surface water withdrawal increased from 707 million gallons per day (Mgal/day) in 1985 to 1140 (Mgal/

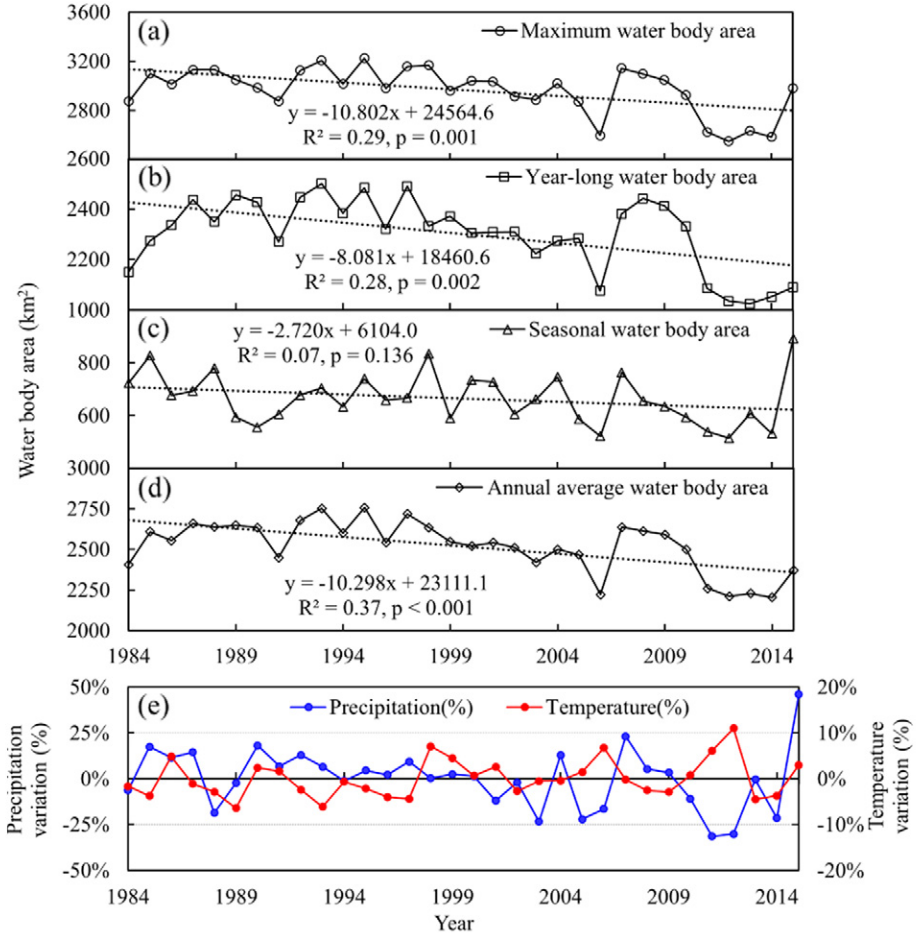

Fig. 3. Inter-annual variations of water body area in different water extents, including maximum (a), year-long (b), seasonal (c), and average (d) water body extents. (e) Statewide annual total precipitation and annual average temperature.

day) in 2010 (U.S. Geological Survey, 2010). The surface water was mainly used for public supply (55%), thermoelectric power (18%), irrigation (13%), and livestock (9%). The surface water withdrawal for public supply, irrigation, and livestock increased gradually from 1985 to 2000 and then decreased gradually from 2000 to 2010. In comparison, the surface water withdrawal for thermoelectric power before 2000 was relatively stable but increased rapidly from 143 (Mgal/day) in 2000 to 384 (Mgal/day) in 2010. Generally, these sectors divert water from year-long water bodies (large lakes, reservoirs, and major rivers), thus having more direct effects on the variability of these large year-long water bodies.

The water body area and number of the previous year had statistically significant positive effects on all six analyses, except the seasonal water body area. The water body extent of one year is gradually changed from the water body extent of the previous year. The water bodies that exist through one year will become the water bodies of the next year, positively affecting the water body extents of the subsequent year. As for seasonal water bodies, they last shorter than 9 months by definition. Thus, seasonal water bodies in one year may

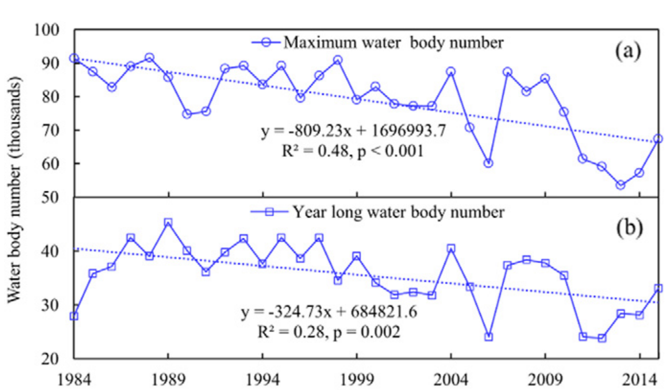

Fig. 4. Inter-annual variations of the number of (a) maximum water bodies and (b) year-long water bodies.

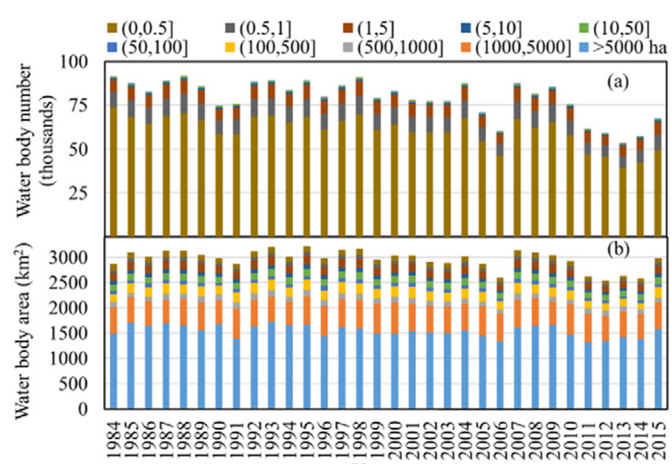

Fig. 5. Water body number and area distribution at different water body size levels, (a) water body number distribution, and (b) water body area distribution.

Table 1
Multiple linear regression analyses of water body area and number with precipitation, temperature and surface water withdrawal in Oklahoma. The six dependent variables are maximum water body area (MWBA), maximum water body number (MWBN), year-long water body area (YWBA), year-long water body number (YWBN), seasonal water body area (SWBA) and annual average water body area (AAWBA). P and T are the statewide annual total precipitation and annual average temperature respectively. SWW is the statewide surface water withdrawal in million gallons per day. $MWBA_p$, $MWBN_p$, $YWBA_p$, $YWBN_p$, $SWBA_p$, and $AAWBA_p$ denote the water body status in the previous year. R^2 is the proportion of variance in the dependent variable which can be explained by the selected explanatory variables. SEE is the standard error of the estimate. F and Sig. are the F-statistic and the p-value associated with it.

Maximum water body area		Maximum water body number		Year-long water body area		Year-long water body number		Seasonal water body area		Annual average water body area	
Variable	Coeff.	Variable	Coeff.	Variable	Coeff.	Variable	Coeff.	Variable	Coeff.	Variable	Coeff.
P	0.76^{***}	P	29.14^{**}	P	0.26^{*}	P	14.65^{***}	P	0.37^{***}	P	0.37^{**}
T		T		T	-57.16^{*}	T	-3038.99^{**}	T		T	-55.87^{*}
SWW		SWW		SWW	-0.23^{*}	SWW	-9.95^{*}	SWW		SWW	-0.30^{*}
$MWBA_p$	0.55^{***}	$MWBN_p$	0.64^{***}	$YWBA_p$	0.48^{***}	$YWBN_p$	0.29^{*}	$SWBA_p$		$AAWBA_p$	0.37^{*}
Constant	644	Constant	286	Constant	2065^{***}	Constant	68535^{***}	Constant	321^{**}	Constant	2396^{**}
Model summary		Model summary		Model summary		Model summary		Model summary		Model summary	
R^2	0.64	R^2	0.59	R^2	0.72	R^2	0.79	R^2	0.36	R^2	0.73
SEE	119	SEE	7160	SEE	81	SEE	2791	SEE	78	SEE	89
F	24.79	F	20.49	F	16.75	F	24.48	F	16.30	F	17.79
Sig.	0.000	Sig.	0.000	Sig.	0.000	Sig.	0.000	Sig.	0.000	Sig.	0.000

* $p < 0.05$.
** $p < 0.01$.
*** $p < 0.001$.

dry up some time within that year and have no significant effects on the water bodies of the subsequent year.

3.3.2. Variation of open surface water bodies in a dry and wet year

Precipitation is one of the most dominant climate drivers of water availability (Bates et al., 2008). Therefore, precipitation has strong effects on the water body area and number. Statewide annual total precipitation in 2006 and 2007 was 780 mm and 1150 mm, respectively. Compared with the average precipitation over the 32 years (934 mm), 2006 was a dry year while 2007 was a wet year. Fig. 6 shows the distribution of statewide water body area and number at the maximum water body extent for 2006 and 2007. In the wet year of 2007, the area and number of water bodies were much larger than those in the dry year of 2006. The number of water bodies in 2006 was about 60,000, which was 27,000 less than that of 2007 (87,000). The additional 27,000 water bodies in 2007 were mainly small water bodies, of which 21,000 were smaller than 0.5 ha, 3000 were between 0.5 and 1 ha, and 2000 were between 1 and 5 ha. Accordingly, the changes in total number of water bodies in each year were mainly caused by changes in the number of small water bodies. The existence and detection of these small water bodies were strongly affected by the amount of precipitation. The maximum water body area in 2006 was about 2596 km^2, which was about 550 km^2 less than that of 2007

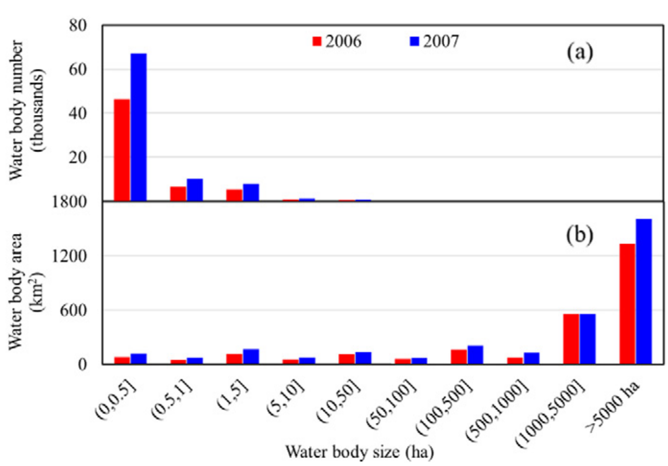

Fig. 6. Water body number and area distribution of the maximum water body extent in a dry (2006) and wet (2007) year, (a) water body number distribution, (b) water body area distribution.

(3143 km^2). Of the additional 550 km^2 water area in 2007, 68% was attributed to the increase in area of 148 large water bodies (>100 ha). Thus, the variability in water body area was mainly caused by variations in the surface area of large water bodies.

4. Discussion

4.1. Advantages and uncertainties of this study

Oklahoma has a large number of small ponds and lakes, and these small water bodies tend to have large temporal variability in extent (i.e., size and water body frequency). In order to characterize the intra-annual and inter-annual variations of the water bodies, we proposed four water body extent related indicators derived from water body frequency maps (maximum = sum area of all effective water body pixels within a year; year-long = pixels covered by water for at least 75% of the year, seasonal = pixels covered by water between 25 and 75% of the year, and average = all the effective water body pixels, weighted by the water body frequency). Together, these indicators captured a more complete picture of the variability of surface water bodies. A recent global water body mapping study provided the time of water presence and location of water change in terms of seasonality and persistence (Pekel et al., 2016). However, because of the global scale involved, Pekel et al. (2016) didn't include such details as the annual change in water body area and number of different water extents, nor any information regarding the annual average water body extent. In addition, our algorithm had a robust performance based on the combined relationships for mNDWI and EVI/NDVI, instead of a certain threshold. The constant thresholds in previous studies could be subjective and time-consuming (Feyisa et al., 2014), and also difficult to extrapolate to other regions due to their variances in different images and locations (Ji et al., 2009).

The classification error of this study was mainly caused by omission error (Table S2 in SOM 7). Omission error was reported greater than commission error in most water indices (Feyisa et al., 2014; Fisher et al., 2016; Li et al., 2013). Mixed pixels at the edge of water bodies could be a major reason for water pixel omission (Fisher et al., 2016). Narrow rivers and streams were often not or only partially detected because of the weak water signal in the mixed pixels (Feng et al., 2016). The major rivers in Oklahoma often have broad, sand-filled channels with active water courses occupying a small portion of the river bed (Johnson and Luza, 2008). Thus, many rivers and streams had low water body frequency in our study and appeared in the seasonal water body maps rather than year-long water body maps. The low albedo surfaces, including asphalt roads, shadows of mountains, buildings, trees, and clouds are the major source for commission error in water classification (Feng et al., 2016; Feyisa et al., 2014; Verpoorter et al., 2012). Although the cloud mask band was applied in data preprocessing, the undetected residual cloud and cloud shadows would still contribute to commission error. The water body frequency threshold (0.25) used here could remove most of the temporal noise out of the water body frequency maps. However, while removing the noise, the frequency threshold also removed some temporary water signals, which may have led to the underestimation of water body area.

4.2. Driving factors of water body changes

Before 2011, anytime the maximum water body area had a drop of >200 km^2 (1996, 1999 and 2006), it began to recover in the following year (see Fig. 3a). However, in 2011, when the maximum water body area dropped 300 km^2, it continued dropping in 2012 and remained low through 2013 and 2014. The shrunken water body area from 2011 to 2014 was very likely caused by the long-lasting drought in Oklahoma from 2011 to 2014 (Hoerling et al., 2014; Kogan and Guo, 2015). In 2012, when the statewide annual precipitation was the second lowest (653 mm) in the last 32 years (Fig. 3e), the maximum water body area was the smallest (2548 km^2). The Southern Great Plains of the US are expected to have more frequent and more intense droughts in the future (Shafer et al., 2014). Thus, there is a higher probability for the total water body area to be smaller and a higher chance for the water body area to decline to a new low record – both issues will pose more challenges to the human society and the affected ecosystems. In addition to the climate-based driving factors, anthropogenic activities, including agricultural irrigation, energy production, consumptive water use and water management can also cause changes in open surface water bodies (Liu et al., 2013; Tao et al., 2015). More analysis regarding the influence of human activities on surface water bodies should be considered in future studies.

This study also indicated that smaller lakes or ponds were more vulnerable in comparison with larger water bodies in drought situations. According to the zonal statistics of the 2015 water body frequency map, water body size had a significant logarithmic relationship with its average water body frequency (SOM 14). Larger water bodies had higher average water body frequencies, indicating that they have higher probabilities to have water throughout the year. On the contrary, smaller water bodies had lower average water body frequencies, meaning that they had a higher risk to completely evaporate sometime during a given year.

4.3. Consequences of water body area shrinkage

Statistically significant downward trends were found in water body area and number over the last 32 years, which indicated the shrinkage of water body area and the gradual vanishing of some water bodies. Open surface water bodies are the major water source for public supply, thermal electric power industry, and livestock production in Oklahoma. The shrinkage of water body area could have a huge influence on Oklahoma's socioeconomic systems. The prolonged drought in 2011 and 2012 reduced the water body area of Oklahoma to a great degree. For example, the water levels of Oklahoma City's Lake Hefner were at an all-time low and water from other lakes had to be siphoned for public supply (Campfield, 2013). Thermoelectric plants depend on surface water for cooling, fuel processing, and emission control. Water withdrawals for thermoelectric power in Oklahoma increased 170% from 2000 to 2010 (U.S. Geological Survey, 2010). The shrinkage of water area could limit the availability of water for withdrawal, expose the water intake structures, and increase water temperatures beyond regulations (Argonne National Laboratory, 2012). Similarly, decreased surface water supplies can threaten Oklahoma's 8 hydroelectric projects, which supplies electricity to about 2 million users across Oklahoma and 5 bordering states (USACE, 2017). The cattle market is the dominant livestock industry in Oklahoma, with approximately 5.5 million cattle and calves on farms and ranches, ranking the state third in the nation for beef cow production (Oklahoma Water Resources Board, 2011). Oklahoma accounts for about 9% of the total freshwater withdrawals for livestock in the US, ranking the state third behind California and Texas (Oklahoma Water Resources Board, 2011). Sixty-five percent of this freshwater in Oklahoma was obtained from open surface water bodies (U.S. Geological Survey, 2010). Oklahoma's livestock industry is sensitive to the availability of water resources, as seen after the 2011 drought, when the number of cattle and calves in 2012 decreased about 20% to 4.2 million compared to 2007 (5.4 million) (USDA-NASS, 2014). Thus, the trends in water variability discovered in this study should be considered in Oklahoma water resource planning, especially in the sectors of public water supply, hydroelectric and thermoelectric power, and livestock.

Oklahoma is one of the most ecologically diverse states in the nation. It is one of the four states to have more than ten Level III ecological regions (Woods et al., 2005). The shrinkage of water area could also pose threats to these diverse ecosystems. The 2011 drought decreased the flow of the Kiamichi River, Little River, and Mountain Fork River in southeastern Oklahoma substantially and changed the typical continuous flow to discontinuous flow, resulting in the creation of a series of shallow pools along the river channels (Atkinson et al., 2014). From 1992 to 2011, the drought-induced reductions in stream flow and surface water area of Kiamichi River had led to a >60% decline in mussel populations (Vaughn et al., 2015). These changes caused the decrease of mussel density and biomass, and a subsequent loss of mussel-provided ecosystem services (Atkinson et al., 2014). There are a large number of small water bodies distributed across the entire state of Oklahoma. A reduction in the size and number of these small water bodies could lead to the loss of wetlands and threaten the aquatic species that depend on these small water bodies for survival. The annual water body frequency map of the last 32 years and the cumulated water body frequency map of 1984 through 2015 could be used to identify vulnerable aquatic ecosystems that may be subject to drying in future drought years. Thus, actions could be taken to protect endangered aquatic species.

5. Conclusions

Oklahoma has the largest number of artificial lakes in the United States. Therefore, this water body variation study is helpful to private and public natural resource managers and improves our understanding of water resource vulnerability in the Southern Great Plains, which is experiencing increased variability in climate. In this study, the Landsat 5 and 7 surface reflectance archive from 1984 through 2015 was used to characterize water body variations at 30 m spatial resolution. Using these data, both the area and number of different water body extent indicators were analyzed to investigate the water body variability and determine trends over the last 32 years. The water body area of the maximum, year-long, and average water extents showed significant downward trends over the last three decades, indicating that open surface water bodies are gradually shrinking in Oklahoma. Statistically significant downtrends were also found in the number of water bodies in the maximum and year-long water extents in the same period, suggesting that water bodies were vanishing annually. Both the water body area and number underwent obvious variations over the study period. The variability in statewide water body area was mainly influenced by changes in the spatial extent of large water bodies, while the variability in the total number of water bodies was mainly influenced by the small water bodies. Precipitation had statistically significant positive effects on water body area and number while temperature had negative effects. Surface water withdrawals mainly impacted the year-long water bodies. The datasets generated by this study can aid planning in the areas of water resource management, agricultural irrigation, livestock production, and ecological conservation.

Acknowledgements

This study was supported in part by research grants from the USDA National Institute of Food and Agriculture (2013-69002), the National Science Foundation (NSF) EPSCoR program (IA-1301789), and the Department of the Interior, United States Geological Survey to AmericaView (G14AP00002), the Key Research Program of Frontier Sciences of the Chinese Academy of Sciences (QYZDB-SSW-DQC005), and the "Thousand Youth Talents Plan". The authors would like to thank the three anonymous reviewers and Co-Editor in Chief Damià Barceló Cullerès for their valuable comments and suggestions on an earlier draft.

Appendix A. Supplementary data

Supplementary data to this article can be found online at http://dx.doi.org/10.1016/j.scitotenv.2017.03.259.

References

Aherne, J., Larssen, T., Cosby, B.J., Dillon, P.J., 2006. Climate variability and forecasting surface water recovery from acidification: modelling drought-induced sulphate release from wetlands. Sci. Total Environ. 365 (1–3):186–199. http://dx.doi.org/10.1016/j.scitotenv.2006.02.041.

Alsdorf, D.E., Rodriguez, E., Lettenmaier, D.P., 2007. Measuring surface water from space. Rev. Geophys. 45 (2):1–24. http://dx.doi.org/10.1029/2006RG000197.

Argonne National Laboratory, 2012. Impacts of Long-term Drought on Power Systems in the U.S. Southwest, Prepared for the U.S. Department of Energy, U.S. DOE, Washington, DC. (Available at https://energy.gov/sites/prod/files/Impacts%20of%20Long-term%20Drought%20on%20Power%20Systems%20in%20the%20US%20Southwest%20%E2%80%93%20July%202012.pdf. Accessed December 27, 2016.).

Atkinson, C.L., Julian, J.P., Vaughn, C.C., 2014. Species and function lost: role of drought in structuring stream communities. Biol. Conserv. 176:30–38. http://dx.doi.org/10.1016/j.biocon.2014.04.029.

Bates, B.C., Kundzewicz, Z.W., Wu, S., Palutikof, J.P., 2008. Climate change and water. Technical paper of the intergovernmental panel on climate change. IPCC Secretariat, Geneva.

Bhagat, V.S., Sonawane, K.R., 2011. Use of Landsat ETM plus data for delineation of water bodies in hilly zones. J. Hydroinf. 13 (4):661–671. http://dx.doi.org/10.2166/hydro.2010.018.

Boland, D.H.P., 1976. Trophic Classification of Lakes Using Landsat-1 (ERTS-1) Multispectral Scanner Data. U.S. Environmental Protection Agency, Office of Research and Development, Corvallis Environmental Research Laboratory, Assessment and Criteria Development, Corvallis, Oregon.

Brown, C., Lall, U., 2006. Water and economic development: the role of variability and a framework for resilience. Nat. Res. Forum 30 (4):306–317. http://dx.doi.org/10.1111/j.1477-8947.2006.00118.x.

Campfield, Z., 2013. Drought Sinks Water Levels at Oklahoma City's Lake Hefner to All-time Low. NewsOK, Oklahoma (Available at http://newsok.com/article/3744544. Accessed December 27, 2016).

Crist, E.P., 1985. A TM tasseled cap equivalent transformation for reflectance factor data. Remote Sens. Environ. 17 (3):301–306. http://dx.doi.org/10.1016/0034-4257(85)90102-6.

Department of the Interior U.S. Geological Survey, 2012. Landsat Ecosystem Disturbance Adaptive Processing System (LEDAPS) Algorithm Description Document. USGS, Washington, D.C. (Available at https://landsat.usgs.gov/sites/default/files/documents/ledaps_add.pdf. Accessed December 10, 2015).

Dong, J.W., et al., 2015. Tracking the dynamics of paddy rice planting area in 1986–2010 through time series Landsat images and phenology-based algorithms. Remote Sens. Environ. 160:99–113. http://dx.doi.org/10.1016/j.rse.2015.01.004.

Du, Z.Q., Bin, L.H., Ling, F., Li, W.B., Tian, W.D., Wang, H.L., Gui, Y.M., Sun, B.Y., Zhang, X.M., 2012. Estimating surface water area changes using time-series Landsat data in the Qingjiang River Basin, China. J. Appl. Remote. Sens. 6:1–16. http://dx.doi.org/10.1117/1.Jrs.6.063609.

Feng, L., Hu, C.M., Chen, X.L., Li, R.F., 2011. Satellite observations make it possible to estimate Poyang Lake's water budget. Environ. Res. Lett. 6 (4):1–7. http://dx.doi.org/10.1088/1748-9326/6/4/044023.

Feng, M., Sexton, J.O., Channan, S., Townshend, J.R., 2016. A global, high-resolution (30-m) inland water body dataset for 2000: first results of a topographic-spectral classification algorithm. Int. J. Digital Earth 9 (2):113–133. http://dx.doi.org/10.1080/17538947.2015.1026420.

Ferguson, I.M., Maxwell, R.M., 2012. Human impacts on terrestrial hydrology: climate change versus pumping and irrigation. Environ. Res. Lett. 7 (4). http://dx.doi.org/10.1088/1748-9326/7/4/044022.

Feyisa, G.L., Meilby, H., Fensholt, R., Proud, S.R., 2014. Automated water extraction index: a new technique for surface water mapping using Landsat imagery. Remote Sens. Environ. 140:23–35. http://dx.doi.org/10.1016/j.rse.2013.08.029.

Fisher, A., Flood, N., Danaher, T., 2016. Comparing Landsat water index methods for automated water classification in eastern Australia. Remote Sens. Environ. 175:167–182. http://dx.doi.org/10.1016/j.rse.2015.12.055.

Fry, J.A., Xian, G., Jin, S., Dewitz, J.A., Homer, C.G., Limin, Y., Barnes, C.A., Herold, N.D., Wickham, J.D., 2011. Completion of the 2006 national land cover database for the conterminous United States. Photogramm. Eng. Remote. Sens. 77 (9), 858–864.

Gibson, A.M., 1981. Oklahoma, A History of Five Centuries. University of Oklahoma Press, Oklahoma.

Gond, V., Bartholome, E., Ouattara, F., Nonguierma, A., Bado, L., 2004. Monitoring and mapping of waters and wetlands in arid regions using the SPOT-4 VEGETATION imaging system. Int. J. Remote Sens. 25 (5):987–1004. http://dx.doi.org/10.1080/0143116031000139908.

Google Earth Engine, 2017. Landsat 5/7 Surface Reflectance Datasets. Google Earth Engine, California (Available at https://explorer.earthengine.google.com/#detail/LEDAPS%2FLE7_L1T_SR. Accessed March 15, 2017).

Hall, J.W., Grey, D., Garrick, D., Fung, F., Brown, C., Dadson, S.J., Sadoff, C.W., 2014. Water security. Coping with the curse of freshwater variability. Science 346 (6208): 429–430. http://dx.doi.org/10.1126/science.1257890.

Hoerling, M., Eischeid, J., Kumar, A., Leung, R., Mariotti, A., Mo, K., Schubert, S., Seager, R., 2014. Causes and predictability of the 2012 Great Plains Drought. Bull. Am. Meteorol. Soc. 95 (2):269–282. http://dx.doi.org/10.1175/BAMS-D-13-00055.1.

Homer, C., Huang, C.Q., Yang, L.M., Wylie, B., Coan, M., 2004. Development of a 2001 National Land-Cover Database for the United States. Photogramm. Eng. Remote. Sens. 70 (7), 829–840.

Homer, C., Dewitz, J., Fry, J., Coan, M., Hossain, N., Larson, C., Herold, N., McKerrow, A., VanDriel, J.N., Wickham, J., 2007. Completion of the 2001 National Land Cover Database for the conterminous United States. Photogramm. Eng. Remote. Sens. 73 (4), 337–341.

Homer, C., Dewitz, J., Yang, L.M., Jin, S., Danielson, P., Xian, G., Coulston, J., Herold, N., Wickham, J., Megown, K., 2015. Completion of the 2011 National Land Cover Database for the conterminous United States—representing a decade of land cover change information. Photogramm. Eng. Remote. Sens. 81 (5):345–354. http://dx.doi.org/10.14358/Pers.81.5.345.

Hui, F.M., Xu, B., Huang, H.B., Yu, Q., Gong, P., 2008. Modelling spatial-temporal change of Poyang Lake using multitemporal Landsat imagery. Int. J. Remote Sens. 29 (20): 5767–5784. http://dx.doi.org/10.1080/01431160802060912.

Ji, L., Zhang, L., Wylie, B., 2009. Analysis of dynamic thresholds for the normalized difference water index. Photogramm. Eng. Remote. Sens. 75 (11):1307–1317. http://dx.doi.org/10.14358/PERS.75.11.1307.

Johnson, K.S., Luza, K.V., 2008. Earth Sciences and Mineral Resources of Oklahoma. Educational Publication EP-9. Oklahoma Geological Survey, Norman, Oklahoma.

Kogan, F., Guo, W., 2015. 2006–2015 mega-drought in the western USA and its monitoring from space data. Geomat. Nat. Haz. Risk 6 (8):651–668. http://dx.doi.org/10.1080/19475705.2015.1079265.

Lehner, B., Döll, P., 2004. Development and validation of a global database of lakes, reservoirs and wetlands. J. Hydrol. 296 (1–4):1–22. http://dx.doi.org/10.1016/j.jhydrol.2004.03.028.

Li, W.B., Du, Z.Q., Ling, F., Zhou, D.B., Wang, H.L., Gui, Y.M., Sun, B.Y., Zhang, X.M., 2013. A comparison of land surface water mapping using the normalized difference water index from TM, ETM plus and ALI. Remote Sens. 5 (11):5530–5549. http://dx.doi.org/10.3390/rs5115530.

Lin, B., Stackhouse, P., Sun, W.B., Hu, Y.X., Liu, Z.Y., Fan, T.F., 2013. Is Oklahoma getting drier? J. Quant. Spectrosc. Radiat. Transf. 122:208–213. http://dx.doi.org/10.1016/j.jqsrt.2012.07.024.

Liu, H.Y., Yin, Y., Piao, S.L., Zhao, F.J., Engels, M., Ciais, P., 2013. Disappearing Lakes in semiarid northern China: drivers and environmental impact. Environ. Sci. Technol. 47 (21):12107–12114. http://dx.doi.org/10.1021/es305298q.

McFeeters, S.K., 1996. The use of the normalized difference water index (NDWI) in the delineation of open water features. Int. J. Remote Sens. 17 (7):1425–1432. http://dx.doi.org/10.1080/01431169608948714.

McPherson, R.A., et al., 2007. Statewide monitoring of the mesoscale environment: a technical update on the Oklahoma Mesonet. J. Atmos. Ocean. Technol. 24 (3):301–321. http://dx.doi.org/10.1175/Jtech1976.1.

Mercier, F., Cazenave, A., Maheu, C., 2002. Interannual lake level fluctuations (1993–1999) in Africa from Topex/Poseidon: connections with ocean-atmosphere interactions over the Indian Ocean. Glob. Planet. Chang. 32 (2–3):141–163. http://dx.doi.org/10.1016/S0921-8181(01)00139-4.

Mueller, N., et al., 2016. Water observations from space: mapping surface water from 25 years of Landsat imagery across Australia. Remote Sens. Environ. 174:341–352. http://dx.doi.org/10.1016/j.rse.2015.11.003.

Necsoiu, M., Dinwiddie, C.L., Walter, G.R., Larsen, A., Stothoff, S.A., 2013. Multi-temporal image analysis of historical aerial photographs and recent satellite imagery reveals evolution of water body surface area and polygonal terrain morphology in Kobuk Valley National Park, Alaska. Environ. Res. Lett. 8 (2). http://dx.doi.org/10.1088/1748-9326/8/2/025007.

Ogilvie, A., Belaud, G., Delenne, C., Bailly, J.S., Bader, J.C., Oleksiak, A., Ferry, L., Martin, D., 2015. Decadal monitoring of the Niger Inner Delta flood dynamics using MODIS optical data. J. Hydrol. 523:368–383. http://dx.doi.org/10.1016/j.jhydrol.2015.01.036.

Oklahoma Climatological Survey, 2016. Oklahoma Statewide Annual Precipitation and Temperature History with 5-year Tendencies 1895–2015, Oklahoma Climatological Survey, Norman, Oklahoma. (Available at http://climate.ok.gov/index.php/climate/climate_trends/precipitation_history_annual_statewide/CD00/prcp/Annual. Accessed May 5, 2016).

Oklahoma Water Resources Board, 2011. Oklahoma Comprehensive Water Plan Supplemental Report, Agricultural Issues & Recommendations. Oklahoma Water Resources Board, Norman, Oklahoma:pp. 1–17 (Available at http://www.owrb.ok.gov/supply/

ocwp/pdf_ocwp/WaterPlanUpdate/draftreports/OCWP_AgriculturalWater_IssuesRecs.pdf. Accessed November 10, 2016).
OWRB, ODWC, 2015. Lakes of Oklahoma. Oklahoma Water Resources Board and Oklahoma Department of Wildlife Conservation, Oklahoma City, US.
Pekel, J.-F., Cottam, A., Gorelick, N., Belward, A.S., 2016. High-resolution mapping of global surface water and its long-term changes. Nature 540 (7633):418–422. http://dx.doi.org/10.1038/nature20584.
Rouse Jr., J.W., Haas, R., Schell, J., Deering, D., 1974. Monitoring vegetation systems in the Great Plains with ERTS. NASA Special Publication. 351, pp. 309–317.
Santoro, M., Wegmuller, U., Lamarche, C., Bontemps, S., Defoumy, P., Arino, O., 2015. Strengths and weaknesses of multi-year Envisat ASAR backscatter measurements to map permanent open water bodies at global scale. Remote Sens. Environ. 171: 185–201. http://dx.doi.org/10.1016/j.rse.2015.10.031.
Shafer, M., Ojima, D., Antle, J.M., Kluck, D., McPherson, R.A., Petersen, S., Scanlon, B., Sherman, K., 2014. Great Plains. In: Melillo, J.M., Richmond, T.C., Yohe, G.W. (Eds.), Climate Change Impacts in the United States: The Third National Climate Assessment. U.S. Global Change Research Program, United States of America, pp. 441–461.
Shine, T., Mesev, V., 2007. Remote sensing and GIS for ephemeral wetland monitoring and sustainability in southern Mauritania. In: Mesev, V. (Ed.), Integration of GIS and Remote Sensing. Wiley & Sons, Ltd., Chichester, West Sussex, England, pp. 269–284.
Tao, S.L., Fang, J.Y., Zhao, X., Zhao, S.Q., Shen, H.H., Hu, H.F., Tang, Z.Y., Wang, Z.H., Guo, Q.H., 2015. Rapid loss of lakes on the Mongolian Plateau. Proc. Natl. Acad. Sci. U. S. A. 112 (7):2281–2286. http://dx.doi.org/10.1073/pnas.1411748112.
Tulbure, M.G., Broich, M., 2013. Spatiotemporal dynamic of surface water bodies using Landsat time-series data from 1999 to 2011. ISPRS J. Photogramm. Remote Sens. 79:44–52. http://dx.doi.org/10.1016/j.isprsjprs.2013.01.010.
Tulbure, M.G., Kininmonth, S., Broich, M., 2014. Spatiotemporal dynamics of surface water networks across a global biodiversity hotspot-implications for conservation. Environ. Res. Lett. 9 (11). http://dx.doi.org/10.1088/1748-9326/9/11/114012.
Tulbure, M.G., Broich, M., Stehman, S.V., Kommareddy, A., 2016. Surface water extent dynamics from three decades of seasonally continuous Landsat time series at subcontinental scale in a semi-arid region. Remote Sens. Environ. 178:142–157. http://dx.doi.org/10.1016/j.rse.2016.02.034.
U.S. Census Bureau, 2010. State Area Measurements and Internal Point Coordinates. U.S. Census Bureau, Suitland, Maryland (Available at http://www.census.gov/geo/reference/state-area.html. Accessed May 24, 2016).
U.S. Geological Survey, 2010. Water use in the United States. U.S. Geological Survey (Reston, Virginia. Available at http://water.usgs.gov/watuse/data/. Accessed September 10, 2016).
USACE, 2017. Tulsa District, US Army Corps of Engineers Hydropower. US Army Corps of Engineers, Washington, D.C. (Available at http://www.swt.usace.army.mil/Missions/Hydropower/. Accessed March 20, 2017).
USDA-NASS, 2014. 2012 Census of Agriculture. United States Department of Agriculture and National Agricultural Statistics Service, Washington, DC:pp. 340–358 (Available at https://www.agcensus.usda.gov/Publications/2012/. Accessed December 20, 2016).
Vaughn, C.C., Atkinson, C.L., Julian, J.P., 2015. Drought-induced changes in flow regimes lead to long-term losses in mussel-provided ecosystem services. Ecol. Evol. 5 (6), 1291–1305.
Verpoorter, C., Kutser, T., Tranvik, L., 2012. Automated mapping of water bodies using Landsat multispectral data. Limnol. Oceanogr. Methods 10:1037–1050. http://dx.doi.org/10.4319/lom.2012.10.1037.
Verpoorter, C., Kutser, T., Seekell, D.A., Tranvik, L.J., 2014. A global inventory of lakes based on high-resolution satellite imagery. Geophys. Res. Lett. 41 (18):6396–6402. http://dx.doi.org/10.1002/2014gl060641.
Vogelmann, J.E., Howard, S.M., Yang, L., Larson, C.R., Wylie, B.K., Van Driel, N., 2001. Completion of the 1990s National Land Cover Data Set for the conterminous United States from Landsat Thematic Mapper data and ancillary data sources. Photogramm. Eng. Remote. Sens. 67 (6).
Woods, A.J., Omernik, J.M., Butler, D.R., Ford, J.G., Henley, J.E., Hoagland, B.W., Arndt, D.S., Moran, B.C., 2005. Ecoregions of Oklahoma, map scale 1:1,250,000. U.S. Geological Survey (Reston, Virginia).
Xiao, X., Boles, S., Frolking, S., Salas, W., Moore, B., Li, C., He, L., Zhao, R., 2002. Observation of flooding and rice transplanting of paddy rice fields at the site to landscape scales in China using VEGETATION sensor data. Int. J. Remote Sens. 23 (15):3009–3022. http://dx.doi.org/10.1080/01431160110107734.
Xiao, X.M., Boles, S., Frolking, S., Li, C.S., Babu, J.Y., Salas, W., Moore, B., 2006. Mapping paddy rice agriculture in South and Southeast Asia using multi-temporal MODIS images. Remote Sens. Environ. 100 (1):95–113. http://dx.doi.org/10.1016/j.rse.2005.10.004.
Xiao, X.M., Boles, S., Liu, J.Y., Zhuang, D.F., Frolking, S., Li, C.S., Salas, W., Moore, B., 2005. Mapping paddy rice agriculture in southern China using multi-temporal MODIS images. Remote Sens. Environ. 95 (4):480–492. http://dx.doi.org/10.1016/j.rse.2004.12.009.
Xu, H.Q., 2006. Modification of normalised difference water index (NDWI) to enhance open water features in remotely sensed imagery. Int. J. Remote Sens. 27 (14): 3025–3033. http://dx.doi.org/10.1080/01431160600589179.